FINITE ELEMENT MODELING OF BINARY ACOUSTIC FRESNEL LENSES

Shiu C. Chan, Mani Mina, S.S. Udpa, W. Lord, L. Udpa and T. Xue
Department of Electrical Engineering and Computer Engineering
Iowa State University
Ames, IA 50011

INTRODUCTION

Binary acoustic Fresnel lenses (BAFLs) have recently emerged as possible replacements for spherical lenses for applications in acoustic microscopy. BAFLs are surface relief structures that are relatively easy to manufacture compared to conventional spherical lenses. While the latter requires careful grinding and polishing, the former can be easily fabricated to sub-micron dimension accuracy using existing VLSI etching technology. The term binary arises from the fact that each masking step during the lens production creates two phase levels. Therefore, a total of 2^n phase levels are created in n masking etching steps. A special case is when $n = 1$ (2 phase levels), which corresponds to the conventional Fresnel lens (zone plate).

Binary lens design is typically based on ray optics (scalar theory). Unfortunately, the scalar theory is inadequate in most cases for predicting the binary lens' field profile, focusing characteristics, and diffraction efficiency [1]-[6]. For example, the ray theory assumption is only valid when the dimensions of the surface relief structure are less than five times the relevant wavelength ($5\lambda_r$). In practice, (particularly in high frequency applications) this requirement is often violated.

A remedy to the deficiency is to use a vector formulation and employ finite element models (FEMs) to simulate the geometry. Such models are not limited by the scalar theory and its assumptions, thus the modeling results provide good approximations to the actual physical behavior of the lenses. These models can serve as valuable tools for designing, analysing, and evaluating lens profiles prior to their fabrication.

BINARY ACOUSTIC FRESNEL LENS

Reflection, refraction, and diffraction are three known mechanisms for redirecting waves. While regular lenses involve both reflection and refraction of energy, Fresnel and binary lenses use the diffractive properties of the structures. The governing equation of these diffractive lenses is the grating equation, and their field profiles are the result of wave interference. Therefore, the lens' phase function is the most important characteristic of a diffractive lens.
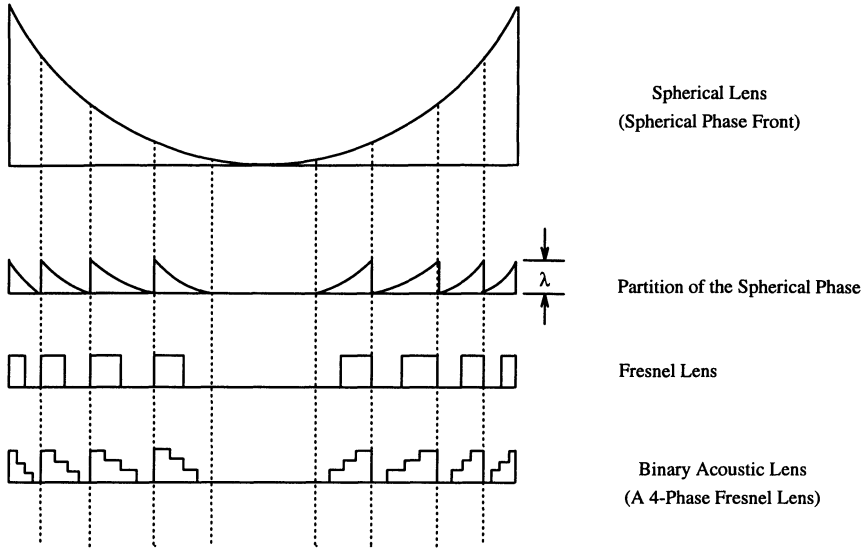
Figure 1. The phase front relationships in a concave lens, a Fresnel lens, and a stair-like binary surface relief structure (a BAFL).

Figure 1 shows the phase profile for a spherical lens, a Fresnel lens and a BAFL. A BAFL is a planar structure with phase levels approximating a spherical phase front. The approximation error decreases as the number of phase levels increases, which also improves the lens efficiency. The least efficient BAFL is the 2-level structure with a maximum efficiency of $\approx 41\%$.

The design and the theoretical first-order diffraction efficiency equations for a N phase level BAFL are given in Figure 2. These equations are based on the ray theory. As the dimensions of the BAFL decreases relative to the wavelength of the acoustic signal, the equations become less accurate. Nevertheless, they can be used, as a first approximation, for designing the BAFLs. The FEM is then employed to simulate the BAFL and estimate the field profile, diffraction efficiency, and focusing characteristics. The estimates can be examined to improve the design of the BAFL subsequently.

FINITE ELEMENT MODELING

The governing equation for waves in a homogeneous, isotropic solid is [7]-[9]

$$c_{ijkl}u_{k,lj} = \rho\ddot{u}_i \qquad (1)$$

where

$$
\begin{aligned}
c_{ijkl} &= \lambda\delta_{ij}\delta_{kl} + \mu(\delta_{ik}\delta_{jl} + \delta_{il}\delta_{jk}) \\
u_i &= \text{displacement vector} \\
\rho &= \text{material volume density} \\
\lambda, \mu &= \text{Lame constants}
\end{aligned}
$$

To solve Eq. 1, we employ finite element formulation in space, and the finite difference method to step forward in time. Additional details of the method are described in [7]-[9].
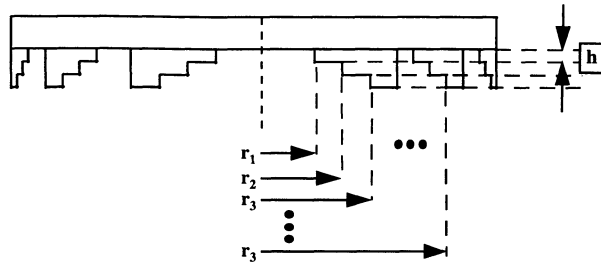
r_k = radius of the kth phase level = $\{ (F_0 + kl /N)^2 - F_0^2 \}^{0.5}$

η_1^N = First order efficiency for N levels = $\left(\dfrac{sin\left(\frac{\pi}{N}\right)}{\left(\frac{\pi}{N}\right)} \right)^2$

h = step height = $\left[N n \left(\dfrac{1}{c_1} - \dfrac{1}{c_2} \right) \right]^{-1}$

N = number of phase levels c_1 = speed in medium 1
F_0 = the focal distance c_2 = speed in medium 2
n = operation frequency

Figure 2. The design equations for an N level BAFL.

Finite Element in Space

The finite element solution [7]-[9] for Eq. 1 involves minimizing a scalar energy functional with respect to nodal displacements. This energy functional is given by

$$
\begin{aligned}
E(u_i, t) &= Potential\ Energy + Kinetic\ Energy - Work\ done\ by\ external\ forces \\
&= P(u_i, t) + K(u_i, t) - W_e(u_i, t)
\end{aligned}
\tag{2}
$$

In the FEM model for the BAFL, the lens structure is an axisymmetric geometry (Figure 2). In this case, the displacement can be approximated in terms of the elemental nodal values as

$$
\mathbf{u}_i^e(r, z, t) = \mathbf{N}_I(r, z, t)\mathbf{U}_{iI}^e(t)
\tag{3}
$$

where

$$
\begin{aligned}
\mathbf{u}_i^e(r, z, t) &= \text{displacement at a point in the element} \\
\mathbf{N}_I(r, z, t) &= \text{shape function} \\
\mathbf{U}_{iI}^e(t) &= \text{nodal displacement}
\end{aligned}
$$

The use of rectangular elements in the FEM implies an 8x1 vector for the nodal displacement values, and a 2x8 matrix for the shape function. This results in a 2x1 vector representing the displacement components in the radial and axial directions.

It can be shown that the solution of the elastic wave equation is the same as the solution for a stationary point of the energy functional. After minimizing the energy functional with respect to the displacement for each element, and assembling the resulting elemental matrix in a global matrix, we obtain

$$
\mathbf{M}\ddot{\mathbf{u}}_t + \mathbf{K}\mathbf{u}_t = \mathbf{R}_t
\tag{4}
$$

where $\mathbf{M}$, $\mathbf{K}$, and $\mathbf{R}$ represent global mass, stiffness and traction force matrices, respectively.
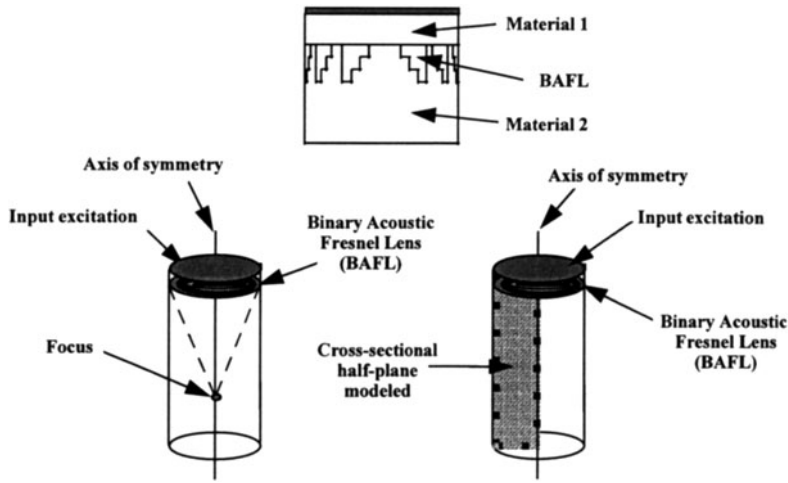
Figure 3. Axisymmetric geometry for the BAFL FEM.

Finite Difference in Time

The finite difference approach is used to obtain the solution of the wave equation in time. Replacing the time derivatives in Eq 4 with their central difference approximation yields [7]-[9]

$$\frac{1}{(\Delta t)^2}\mathbf{M}\mathbf{u}_{t+\Delta t} = \mathbf{R}_t - \mathbf{K}\mathbf{u}_t + \frac{2}{(\Delta t)^2}\mathbf{M}\mathbf{u}_t - \frac{1}{(\Delta t)^2}\mathbf{M}\mathbf{u}_{t-\Delta t} \qquad (5)$$

When obtaining the explicit solution for the displacements, the technique of mass lumping (summarized in Eq. 6) is used for computational facility in inverting the global mass matrix.

$$\mathbf{M}_{JI}^{diag} = \begin{cases} \alpha\mathbf{M}_{IJ} & \text{if} I = J \\ 0 & \text{if} I \neq J \end{cases} \qquad (6)$$

$$\alpha = \frac{\sum_I \sum_J \mathbf{M}_{IJ}}{\sum_I \mathbf{M}_{II}}$$

The final equation modeled by the FEM is:

$$\mathbf{u}_{t+\Delta t} = (\Delta t)^2 (\mathbf{M}^{diag})^{-1}\mathbf{R}_t - \mathbf{K}(\Delta t)^2 (\mathbf{M}^{diag})^{-1}\mathbf{u}_t + \mathbf{u}_t - \mathbf{u}_{t-\Delta t} \qquad (7)$$

RESULTS

The test geometry for the BAFL model is shown in Figure 3. The axisymmetric nature of the geometry is exploited to confine the modeling to the plane of symmetry. The simulation results show the wave propagating on the cross-sectional half-plane as indicated in Figure 3.

Table 1 contains the mesh and time discretization details of the FEM model used for simulating the 4-, 8-, and 16-level BAFLs. All three lenses are designed to have the same diameter and focal distance. The elements of the FEM are rectangular

Table 1. Design details for the 4-, 8-, and 16-level BAFL FEMs.

| Attributes		4-level BAFL	8-level BAFL	16-level BAFL
FE Mesh Information	No. Radial Elems.	252	272	314
	No. Long. Elems.	921	941	945
Phase Zone Information	Smallest Ring Size	$790\mu m$	$392\mu m$	$195\mu m$
	Largest Ring Size	5.79mm	4.09mm	2.89mm
Time Scale Information	No. Time Steps	7876	10501	10501
	Time Step Size	6.0ns	4.5ns	4.5ns
Physical Sizes	Lens Diameter	4.74cm	4.74cm	4.74cm
	Focal Length	5.0cm	5.0cm	5.0cm
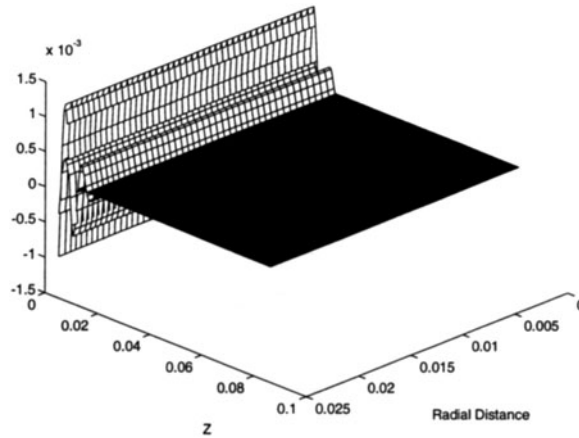
Figure 4. Simulated input plane wave.

with variable sizes in the axial and radial directions. The input signal to the lens structure is a plane wave with respect to the lens. However, in the time domain, the input waveform follows a raised-cosine function with a center frequency of 1 MHz. Figure 4 shows the simulated input plane wave before entering the BAFL region used in the 4-, 8-, and 16-level lens simulations.

The lens substrate (material 1) is quartz with longitudinal velocity $V_l = 5970\text{ms}^{-1}$, shear velocity $V_s = 3765\text{ms}^{-1}$ and density $\rho = 2200\text{gm}^{-3}$. The coupling medium (material 2) is a generic material used to observe the propagation of the shear and longitudinal wave. This medium has $V_l = 1490\text{ms}^{-1}$, $V_s = 894\text{ms}^{-1}$, and $\rho = 1000\text{gm}^{-3}$.

Figures 5, 6, and 7 show the focusing effects for the 4-, 8-, and 16-level BAFLs, respectively. These results demonstrate the interference of the phase shifted plane waves as they propagate along the coupling medium. The focusing effect can be explained as a directional interference pattern that is maximized at the focal point. This phenomenon can be observed at the focal area, at which the concentration of energy is made up of planar waves that have interfered in the vicinity. Minor side lobes with energy content that are less than that of the main lobe are also observed at the focal plane.
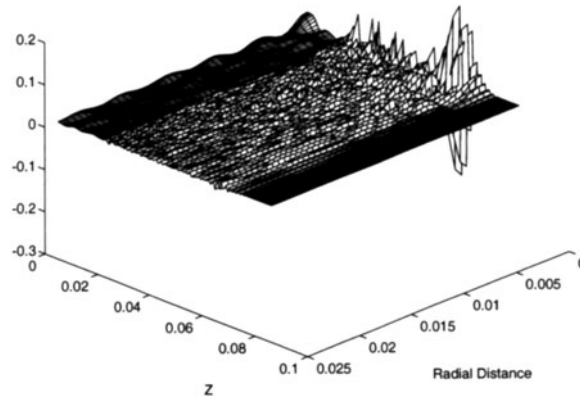
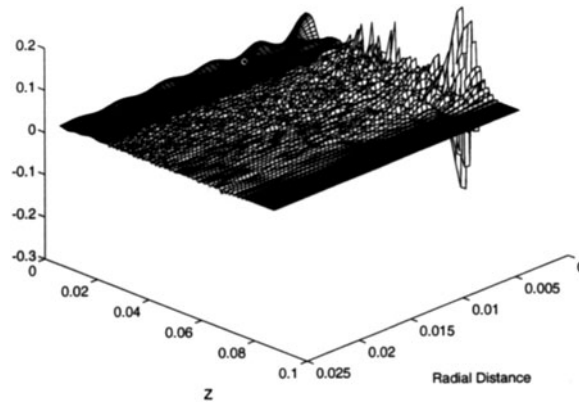Figure 5. Focusing effect for the 4 levels BAFL.

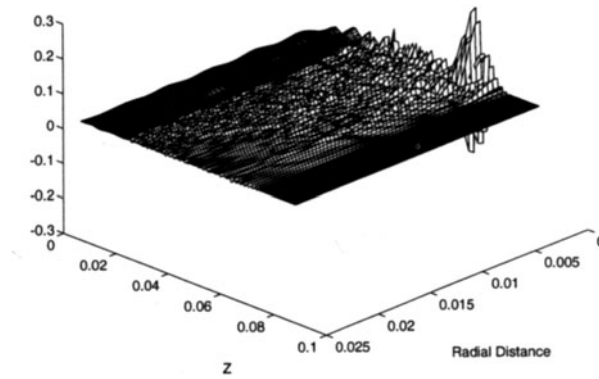
Figure 6. Focusing effect for the 8 levels BAFL.

Figure 7. Focusing effect for the 16 levels BAFL.

Table 2. Diffraction efficiencies obtained from using the equation shown in Figure 2 and the method described in text.

	4-level BAFL	8-level BAFL	16-level BAFL
Ray Theory (Fig. 2)	0.81	0.95	0.99
FE modeling results	0.81	0.81	0.81

Diffraction Efficiency

Theoretically, the first-order diffraction efficiency of a BAFL is defined under continuous wave (CW) conditions as the percentage of the input energy diverted towards the lens' focal point. However, since the model simulates transient conditions, the following algorithm is used for calculating efficiency.

1. Locate the focal plane parallel to the lens.

2. Calculate the total energy in the focal plane.

3. Calculate the full width half maximum (FWHM) energy in the focal region.

4. Obtain the efficiency as the ratio of results obtained in step 3 and step 2.

Table 2 shows the theoretical and numerical diffraction efficiencies obtained using the equation shown in Figure 2 and the finite element simulations, respectively. Since the two diffraction efficiencies are calculated using two different approaches, and recognizing that the model does not simulate true continuous-wave input conditions, the two sets of results should strictly not be compared. The large disagreement however indicates the limitations of the ray theory approach in predicting performance particularly when the dimensions of the surface relief structures are comparable to the wavelength. The simulation results show that, for the BAFL structures modeled, increasing the phase divisions from 4 to 8 and 16 levels does not improve the performance of the lens structures as predicted by the efficiency equation in Figure 2. Consequently, for the given diameter, focal length and operating frequency (1 MHz), we conclude that optimal performance is achieved with a 4-level BAFL, and increasing the number of levels does not improve efficiency.

The results also demonstrate the capabilities of the FEMs in characterizing the propagation of elastic waves in the lens substrate and the coupling medium.

CONCLUSIONS

Current BAFL designs are based on equations developed from the ray theory. In many acoustic microscopy applications, the ray theory is not applicable for characterizing BAFLs. Due to this deficiency, FEMs have been developed to study these lenses. These models are capable of simulating and characterizing the beam-forming and focusing power of the lenses, as well as displaying their underlying focusing mechanism: the diffraction and interference of the input waves. Modeling results show that FEMs can serve as valuable tools for the study and evaluation of BAFLs prior to their fabrication.

ACKNOWLEDGMENTS

REFERENCES

1 G.J. Swanson, "Binary Optics Technology: The Theory and Design of Multi-level Diffractive Optical Elements," *Technical Report No. 854,* Lincoln Laboratory, Lexington, Massachusetts:MIT, August 14, 1989.

2 Gary J. Swanson and Wilfrid B. Veldkamp, "Infrared applications of diffractive optical elments," *Proc. SPIE: Holographic Optics:Design and Applications,* Vol. 883, 1988, pp.155-162.

3 J.R. Leger, M. Holz, G.J. Swanson, and W.B. Veldkamp, "Coherent Laser Beam Addition: An Application of Binary-Optics Technology," *The Lincoln Laboratory Journal,* Vol. 1, No. 2, 1988, pp.225-245.

4 B. Hadimioglu, E.G. Rawson, R. Lujan, M. Lim, J.C. Zesch, B.T. Khuri-Yakub and C.F. Quate, "High-efficiency Fresnel Acoustic Lenses," *IEEE Ultrasonics Symposium,* 1993, pp.579-582.

5 S.A. Farnow, "Acoustic Applications of the Zone Plate," Ph.D. Dissertation, Stanford University, 1975.

6 G.J. Swanson, "Binary Optics Technology: Theoritical Limits on the Diffraction Efficiency of Multilevel Diffractive Optical Elements," *Technical Report No. 914,* Lincoln Laboratory, Lexington, Massachusetts:MIT, March 1, 1991.

7 W. Lord, R. Ludwig, and Z. You, "Developments in ultrasonic modeling with finite element analysis," Journal of Nondestructive Evaluations, Vol. 9, pp.129-143, 1990.

8 R. Ludwig and W. Lord, "Finite element study of ultrasonic wave propagation and scattering in an aluminum block," Mat. Eval., Vol. 46, pp.108-113, 1988.

9 R. Ludwig and W. Lord, "A finite element formulation for the study of ultrasonic NDT systems," IEEE Trans. UFFC, Vol. 35, pp.809-820, 1988.